

## Shell model calculations in the lead region: $^{205}\text{Hg}$ , $^{205}\text{Tl}$ , $^{211}\text{Po}$ , and $^{211}\text{Bi}$

B. Silvestre-Brac and J. P. Boisson

*Institut des Sciences Nucléaires, 53 Avenue des Martyrs, 38026 Grenoble-Cédex, France*

(Received 20 November 1980)

Exact shell model calculations for nuclei consisting of three nonidentical particles outside the  $^{208}\text{Pb}$  closed shell core have been performed using a basis that contains correlated pairs. Two kinds of effective interactions are tested and the results are compared with the experiment. The possibility of high spin isomeric states is suggested for nuclei studied.

[NUCLEAR STRUCTURE  $^{205}\text{Hg}$ ,  $^{205}\text{Tl}$ ,  $^{211}\text{Po}$ ,  $^{211}\text{Bi}$ ; calculated levels  $J$ ,  $\pi$  and spectroscopic factors. Kuo-Herling and Kim-Rasmussen interactions.]

### I. INTRODUCTION

The doubly magic  $^{208}\text{Pb}$  nucleus is known to be a very good inert core and hence the nuclei in the lead region are interesting cases for shell-model calculations. However, the number of shells to be taken into account is rather large and the "standard" shell model procedure,<sup>1</sup> using individual particle wave functions and fractional parentage coefficients, rapidly becomes inoperative with increasing particle number. One of the most complete treatments in this conventional framework is the study of McGrory and Kuo<sup>2</sup> concerning nuclei with three and four identical particles outside the  $^{208}\text{Pb}$  core. These authors included in their calculations six proton orbits; however, they only used five neutron orbits and were obliged to renormalize the neutron-neutron interaction, which had been derived originally by using seven neutron orbits.

An alternative way to solve the shell-model equations is to use a weak-coupling basis.<sup>3</sup> This is a very appealing method since the basis states already contain a part of the two-body correlation, and this allows a drastic truncation in the diagonalization space.<sup>4</sup> Nevertheless this is not the only advantage of the weak-coupling method (WCM). Within this scheme and thanks to a new method of calculating matrix elements, which we have used previously,<sup>4</sup> it is possible to solve the shell-model problem exactly without too much computational effort for cases where standard shell-model calculations have not yet been made. For example, we have been able to treat exactly the  $^{211}\text{Pb}$ , which is a three-neutron system including seven neutron orbits.<sup>4</sup> In order to achieve a systematic theoretical study of nuclei in the lead region, we present in this paper an exact shell-model treatment (using the weak coupling basis) for systems containing three nonidentical particles outside the  $^{208}\text{Pb}$  core, namely  $^{205}\text{Hg}$ ,  $^{205}\text{Tl}$ ,  $^{211}\text{Po}$ , and  $^{211}\text{Bi}$  nuclei. Until now almost no theoretical

work has been devoted to these nuclei. Moreover, the theoretical studies to date considered only one shell for each type of particle<sup>5,6</sup> or drastically truncated the two-particle space (phonons),<sup>7</sup> or have used macroscopic phonons.<sup>8</sup> The aim of our more microscopic and complete calculations is twofold: to be able to test the known proton-neutron effective interactions when enough experimental data is available and to provide a partial background for future experimental studies when experimental data is scarce, and thus fill a gap with respect to previous simpler calculations.

In the next section, the formalism necessary to treat this problem is developed. In Sec. III we discuss in detail the two different effective interactions used in this paper and the configuration space relative to each one. In Sec. IV applications to  $^{205}\text{Hg}$ ,  $^{205}\text{Tl}$ ,  $^{211}\text{Po}$ , and  $^{211}\text{Bi}$  nuclei are presented and finally conclusions are drawn in the last section.

### II. FORMALISM

The formalism we use to deal with the weak-coupling basis has been developed in detail in Sec. II of Ref. 4. Here we focus our attention on the discussion of the overlap matrix  $\Delta$  and of the dynamical matrix  $A$  [see Eqs. (2.4) and (2.6) of Ref. 4].

Here we will analyze a nucleus consisting of three-nonidentical particles outside a closed shell core and neglect core excitations. In the following  $|0\rangle$  is the inert core wave function and  $C_m^\dagger(k)$  [ $C_m(k)$ ] the creation (annihilation) operators for a particle (or a hole) of type  $k$  ( $k$  standing for neutron or proton) in an orbit  $m$ . As known from standard quantum mechanics, one can use either anticommutation or commutation relations for operators concerning two different kinds of particles. Anticommutation rules will be employed from now on for convenience.

$$\begin{aligned} \{C_m(k), C_n(k')\} &= 0 = \{C_m^\dagger(k), C_n^\dagger(k')\}, \\ \{C_m(k), C_n^\dagger(k')\} &= \delta_{kk'} \delta_{mn} \end{aligned} \quad (2.1)$$

Let us consider the system composed of two particles of kind  $k$  and one particle of kind  $k' \neq k$ . Following the idea of the WCM, two different types of phonons naturally occur—the pairing phonon for the even-even nucleus described by the Tamm-Dancoff (TDA) creation operator

$$P_{\alpha J N}^\dagger(kk) \equiv P_{\alpha J N}^\dagger(k^2) = \frac{1}{2} \sum_{m,n} \langle \alpha J(k^2) | m(k)n(k) \rangle^* \times [C_m^\dagger(k)C_n^\dagger(k)]_{JN} \quad (2.2)$$

and the phonon for the odd-odd nucleus

$$P_{\alpha J N}^\dagger(kk') = P_{\alpha J N}^\dagger(k'k) = \sum_{m,n} \langle \alpha J(kk') | m(k)n(k') \rangle^* \times [C_m^\dagger(k)C_n^\dagger(k')]_{JN}. \quad (2.3)$$

The eigenenergies  $\omega_{\alpha J}$  and the amplitudes  $\langle \alpha J | mn \rangle$  of these phonons are provided by the TDA equations

$$\begin{aligned} [\omega_{\alpha J}(kk) - \epsilon_m(k) - \epsilon_n(k)] \langle \alpha J(k^2) | m(k)n(k) \rangle \\ = \frac{1}{2} \sum_{p,q} (1 + \delta_{pq})^{1/2} (1 + \delta_{mn})^{1/2} \langle p(k)q(k); J | V | m(k)n(k); J \rangle \langle \alpha J(k^2) | p(k)n(k) \rangle \end{aligned} \quad (2.4)$$

and

$$[\omega_{\alpha J}(kk') - \epsilon_m(k) - \epsilon_n(k')] \langle \alpha J(kk') | m(k)n(k') \rangle = \sum_{p,q} \langle p(k)q(k'); J | V | m(k)n(k'); J \rangle \langle \alpha J(kk') | p(k)q(k') \rangle, \quad (2.5)$$

where  $\epsilon_m(k)$  is the single particle energy for a particle of type  $k$ .

From definitions (2.2) and (2.3) it can be seen that a symmetry relation can be imposed on the amplitudes  $\langle \alpha J | mn \rangle = \langle 0 | P_{\alpha J} [C_m^\dagger C_n^\dagger]_J | 0 \rangle$ , i. e.,

$$\begin{aligned} \langle \alpha J(kk') | m(k)n(k') \rangle \\ = (-1)^{j_m + j_{n'} + j + 1} \langle \alpha J(kk') | n(k')m(k) \rangle. \end{aligned} \quad (2.6)$$

One can now imagine two different kinds of WCM basis states for the three nonidentical-particle system, namely

$$\begin{aligned} \text{type (1) basis } |\phi_i^{(1)}\rangle &= |m(k')\alpha J(k^2); IM\rangle \\ &= [C_m^\dagger(k')P_{\alpha J}^\dagger(k^2)]_{IM} | 0 \rangle, \end{aligned} \quad (2.7)$$

$$\begin{aligned} \text{type (2) basis } |\phi_i^{(2)}\rangle &= |m(k)\alpha J(kk'); IM\rangle \\ &= [C_m^\dagger(k)P_{\alpha J}^\dagger(kk')]_{IM} | 0 \rangle. \end{aligned} \quad (2.8)$$

Basis (1) is specially interesting because it is complete and orthonormalized

$$\sum_{m,\alpha,J,I,M} |m(k')\alpha J(k^2); IM\rangle \langle m(k')\alpha J(k^2); IM| = \hat{1}, \quad (2.9)$$

where  $\hat{1}$  is the unit operator in the configuration space.

There is thus no need for an orthonormalization procedure in this case. On the other hand, basis (2) is overcomplete and satisfies the relation

$$\sum_{m,\alpha,J,I,M} \frac{1}{2} |m(k)\alpha J(kk'); IM\rangle \langle m(k)\alpha J(kk'); IM| = \hat{1}. \quad (2.10)$$

Nevertheless the use of both  $|\phi^{(1)}\rangle$  and  $|\phi^{(2)}\rangle$  states may be convenient if the shell-model space has to be truncated. Indeed, in the case of a state strongly populated by a direct one-nucleon transfer reaction from a neighboring odd-odd nucleus,  $|\phi^{(2)}\rangle$  basis vectors should be important in the wave function.

From Eqs. (2.7) and (2.8) are derived the overlap matrices

$$\Delta_{ij}^{(u,v)} = \langle \phi_i^{(u)} | \phi_j^{(v)} \rangle \quad u, v = 1, 2. \quad (2.11)$$

They read explicitly

$$\Delta_{m'(k')\alpha'J'(k^2), m(k)\alpha J(k^2)}^{(11)}(I) = \delta_{mm'} \delta_{\alpha\alpha'} \delta_{JJ'},$$

$$\Delta_{m'(k')\alpha'J'(k^2), m(k)\alpha J(kk')}^{(12)}(I)$$

$$= [\Delta_{m(k)\alpha J(kk'), m'(k')\alpha'J'(k^2)}^{(21)}(I)]^*$$

$$= \sum_{p(k)} M_{p(k)} [m(k)\alpha J(kk'), m'(k')\alpha'J'(k^2); I], \quad (2.12)$$

$$\Delta_{m'(k)\alpha'J'(kk'), m(k)\alpha J(kk')}^{(22)}(I) = \delta_{mm'} \delta_{\alpha\alpha'} \delta_{JJ'} + \sum_{p(k')} M_{p(k')} [m(k)\alpha J(kk'), m'(k)\alpha'J'(kk'); I],$$

where we introduce the following quantity (the indices  $k$  and  $k'$  are omitted in order to simplify the writing).

$$M_p [m\alpha J, m'\alpha'J'; I] = \hat{J}\hat{J} \left\{ \begin{matrix} j_m & j_p & J' \\ j_{m'} & I & J \end{matrix} \right\} \langle \alpha J | pm \rangle^* \langle \alpha' J' | p m' \rangle. \quad (2.13)$$

Writing down the TDA equation for three nonidentical-particle system and using TDA equations (2.4) and (2.5) in order to eliminate the bare-two-body-matrix elements, one obtains the dynamical equations

$$H | \phi_i^{(u)} \rangle = \sum_{\nu=1}^2 \sum_l A_{li}^{(uv)} | \phi_l^{(\nu)} \rangle. \quad (2.14)$$

In turn the matrices  $A$  are given by

$$\begin{aligned} A_{m(k')\alpha J(k^2), m'(k')\alpha'J'(k^2)}^{(11)}(I) &= [\epsilon_m(k') + \omega_{\alpha J}(k^2)] \delta_{mm'} \delta_{\alpha\alpha'} \delta_{JJ'}, \\ A_{m(k')\alpha J(k^2), m'(k)\alpha'J'(kk')}^{(12)}(I) &= \sum_{p(k)} [\omega_{\alpha'J'}(kk') - \epsilon_m(k') - \epsilon_p(k)] M_{p(k)}^* [m'(k)\alpha'J'(kk'), m(k')\alpha J(k^2); I], \\ A_{m(k)\alpha J(kk'), m'(k')\alpha'J'(k^2)}^{(21)}(I) &= \sum_{p(k)} [\omega_{\alpha'J'}(k^2) - \epsilon_m(k) - \epsilon_p(k)] M_{p(k)} [m(k)\alpha J(kk'), m'(k')\alpha'J'(k^2); I], \\ A_{m(k)\alpha J(kk'), m'(k)\alpha'J'(kk')}^{(22)}(I) &= [\epsilon_m(k) + \omega_{\alpha J}(kk')] \delta_{mm'} \delta_{\alpha\alpha'} \delta_{JJ'} + \sum_{p(k')} [\omega_{\alpha'J'}(kk') - \epsilon_m(k) - \epsilon_p(k')] \\ &\quad \times M_{p(k')} [m(k)\alpha J(kk'), m'(k)\alpha'J'(kk'); I]. \end{aligned} \quad (2.15)$$

As in the case of three identical-particle systems, the matrices  $A$  and  $\Delta$  are very similar and this property is used for reducing the numerical effort. Unlike the overlap matrix  $\Delta$ , the dynamical matrix  $A$  is not Hermitian. Moreover, let us point out that even if only one type of basis is used [type (1) or type (2)], for diagonalizing the Hamiltonian, the other type has to be employed as "intermediate states" in the calculation of matrix elements  $\langle \phi_i^{(u)} | H | \phi_j^{(u)} \rangle$ . This is clear from Eq. (2.14).

The normalized three nonidentical particle states

$$| \beta(k^2 k'); IM \rangle = P_{\beta IM}^\dagger (k^2 k') | 0 \rangle = \sum_{u=1}^2 \sum_j X_{j(u)}^{\beta I} | \phi_j^{(u)} \rangle \quad (2.16)$$

are obtained by the procedure described in Sec. II of Ref. 4. The components  $X$  of the wave function are not observable; on the other hand, the scalar products  $\langle \beta | \phi_i \rangle$  which can be used to test the wave functions are related to experimental quantities. Indeed

$$S_{m(k')} [\alpha J(k^2) \rightarrow \beta I(k^2 k')] = | \langle \beta I(k^2 k') | m(k') \alpha J(k^2); I \rangle |^2 \quad (2.17)$$

represents the spectroscopic factor for the trans-

fer to the state  $|\beta I\rangle$  of a particle of type  $k'$  in orbit  $m$  from the state  $|\alpha J\rangle$  of the even even nucleus. In the same way

$$S_{m(k)} [\alpha J(kk') \rightarrow \beta I(k^2 k')] = | \langle \beta I(k^2 k') | m(k) \alpha J(kk'); I \rangle |^2 \quad (2.18)$$

is the spectroscopic factor for the transfer of a particle of type  $k$  from the odd-odd nucleus. Sum rules are deduced from the various "closure" relations [for example, Eqs. (2.9) and (2.10)].

$$\sum_{m\alpha J} S_{m(k')} [\alpha J(k^2) \rightarrow \beta I(k^2 k')] = 1, \quad (2.19a)$$

$$\sum_{\beta} S_{m(k')} [\alpha J(k^2) \rightarrow \beta I(k^2 k')] = 1, \quad (2.19b)$$

$$\sum_{m\alpha J} S_{m(k)} [\alpha J(kk') \rightarrow \beta I(k^2 k')] = 2, \quad (2.19c)$$

$$\begin{aligned} \sum_{\beta} S_{m(k)} [\alpha J(kk') \rightarrow \beta I(k^2 k')] \\ = \Delta_{m(k)\alpha J(kk'), m(k)\alpha'J'(kk')}^{(22)}(I). \end{aligned} \quad (2.19d)$$

### III. CONFIGURATION AND MATRIX ELEMENTS

The configuration space is determined by a given set of active single-particle orbits and the number and type of the valence particles. The

effective two-body interaction is calculated or fitted with some set of active orbits and to be coherent further calculations using this force must be performed within the same set of orbits.

The Kuo and Herling (KH) interaction<sup>9</sup> has proved to be rather good in explaining properties of three identical-nucleon system<sup>4</sup> and in this paper it is used to test the neutron-proton matrix elements. The configuration space is built with seven neutron and six proton single-particle orbits, six neutron and five proton single-hole orbits and these are shown in Fig. 1(a). In Kuo and Herling's work the effective interaction was obtained from the Hamada-Johnston potential through a Brueckner treatment. Three approximations were reported in literature: KH1 corresponding to the bare matrix elements, KH2 including core polarization, i. e.,  $3p-1h$  excitations in intermediate states, KH3 being KH2 plus  $4p-2h$  excitations. In fact, KH3 and KH2 are different for  $0^+$  states and almost identical for other states. It appeared<sup>2</sup> that KH2 was the best approximation for explaining the properties of nuclei in the lead region. It will be used for all types of interactions except for the neutron hole-neutron hole interaction, where the modified force  $KHM = 0.75 KH2 + 0.25 KH1$  has proved to be much better.<sup>2</sup>

In order to see the sensitivity of the results with respect to the two-body interaction, we repeat some calculations with the Kim-Rasmussen (KR) force.<sup>10</sup> The Kim-Rasmussen effective interaction is composed of a central potential and a tensor potential with Gaussian form factors. Originally<sup>10</sup> the various parameters were more or less adjusted to energy levels of  $^{210}\text{Po}$  for the proton-proton system and of  $^{210}\text{Bi}$  for the proton-neutron system. However, there

were some inconsistencies in the configuration set since three single-particle-proton orbits were used for the proton-proton interaction while only two were used for the proton-neutron interaction. Moreover, the tensor part was included only for diagonal elements in the proton-proton system, whereas some nondiagonal elements of the proton-neutron system were needed for the tensor part.

In order to achieve some coherence in the configuration space, we make two different calculations of  $^{210}\text{Bi}$  using the same set of parameters, one with the tensor potential included in the diagonal matrix elements only and the other one with the tensor potential included in all matrix elements. It appeared that the second one is better able to reproduce the  $1^-$  ground state at the right energy. Enlarging configuration space from two to three-proton orbits makes little change in the low-lying spectrum except for a few states. So, for the calculations presented in this paper, we adopt three-proton and seven-neutron orbits, the tensor part being used for all matrix elements in  $^{210}\text{Bi}$  and only for the diagonal elements in  $^{210}\text{Po}$ .

The set of parameters is that given in the original paper of Kim and Rasmussen.<sup>10</sup> With this set, the  $0^+$  states of the neutron-neutron system are very badly described (the ground state of  $^{210}\text{Pb}$  is overbound by some 620 keV with respect to the experimental value). For this reason the  $^{211}\text{Bi}$  nucleus was not studied with the KR force.

It has been claimed that KR parameters can be employed for the hole orbits as well.<sup>11</sup> In fact, two proton-hole orbits and five neutron-hole orbits were used. In this case the tensor part was included only in the diagonal matrix elements. Here again the  $0^+$  states of the even-even nuclei are rather poorly described (the ground states are overbound by 480 keV for  $^{206}\text{Hg}$  and 360 keV for  $^{206}\text{Pb}$ ). It appears also that the  $0^+$  states are very sensitive to the amount of configuration mixing and hence to the number of single particle orbits taken into account.

The configuration set chosen for the KR force is shown in Fig. 1(b). Since the number of single-particle orbits is less for the KR interaction than for the KH one, some states are missing in the KR spectrum compared to that of KH. Moreover, the correspondance between the states obtained from each type of effective interaction is not always easy to establish.

Schiffer and True<sup>40</sup> derived, from experimental data, a two range nucleon-nucleon effective interaction independent of any configuration set. Unfortunately, from a theoretical point of view, most of the physical quantities depend upon such a configuration set. For this reason, we decide

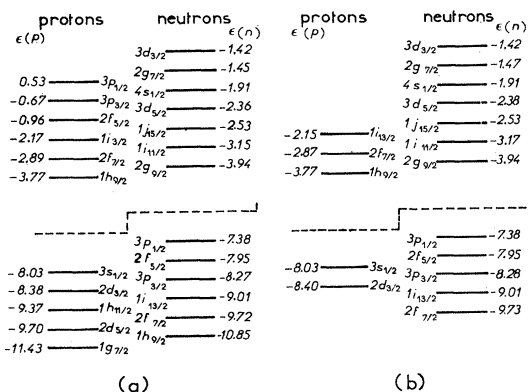


FIG. 1. Configuration set used in our calculations with KH force (a) and KR force (b). The single particle energies  $\epsilon$  are expressed in MeV with respect to the  $^{208}\text{Pb}$  close shell one.

not to use the Schiffer and True effective interaction.

#### IV. APPLICATIONS

As an application of this formalism we investigated the microscopic structure of four nuclei in the lead region, namely  $^{205}\text{Hg}$  (two proton-hole, one neutron-hole),  $^{205}\text{Tl}$  (two neutron-hole, one proton-hole),  $^{211}\text{Po}$  (two protons, one neutron), and  $^{211}\text{Bi}$  (two neutrons, one proton). Since, in this paper, we were interested in an exact shell-model treatment, it was convenient to consider, as basis states for the diagonalization, vectors of type (1) only [see (2.7)]. This avoided an unnecessary orthonormalization procedure. As already pointed out, type (2) vectors are, however, necessary ingredients for calculating the matrix elements  $\langle \phi_i^{(1)} | H | \phi_j^{(1)} \rangle$ . In this case the components of the wave function  $X_{j(1)}^{\beta I}$  are unique (since the basis is complete) and equal to the spectroscopic amplitudes  $\langle \beta I | \phi_j^{(1)} \rangle$  (since the basis is orthonormalized).

The major part of computational time does not lie in the diagonalization procedure but in the evaluation of matrix elements. As has been emphasized in our previous paper,<sup>4</sup> the main interest of our method is the procedure used for calculating the matrix elements. This method is specially suited for systems with few valence particles but with a large number of active orbits, which is the case in the lead region. For such nuclei, shell model calculations have never been made in the configuration spaces built up from all the active orbits of Fig. 1. The maximum dimensions of the matrices to be diagonalized are shown in Table I for the nuclei studied in these spaces using both interactions.

In the following spectra and tables, we shall always refer to the theoretical energies with respect to the experimental ground state energy. In general the low-lying part of the spectrum is much more poorly described in this absolute scale as compared to a relative scale, while the high-lying levels tend to be better reproduced. This is

TABLE I. Maximum sizes of the dimension of the configuration spaces built on orbits of Fig. 1 for the four nuclei studied.

	$^{205}\text{Hg}$	$^{205}\text{Tl}$	$^{211}\text{Po}$	$^{211}\text{Bi}$
KH	$J \begin{matrix} 7^- \\ 2 \end{matrix}$	$J \begin{matrix} 7^+ \\ 2 \end{matrix}$	$J \begin{matrix} 9^+ \\ 2 \end{matrix}$	$J \begin{matrix} 9^- \\ 2 \end{matrix}$
	$n \quad 147$	$n \quad 191$	$n \quad 296$	$n \quad 371$
KR	$J \begin{matrix} 5^- & 3^- \\ 2 & 2 \end{matrix}$	$J \begin{matrix} 5^+ \\ 2 \end{matrix}$	$J \begin{matrix} 9^+ & 11^+ \\ 2 & 2 \end{matrix}$	not studied in this paper
	$n \quad 13$	$n \quad 38$	$n \quad 108$	

mainly due to the description of the collective states—especially the  $0^+$  ground state—in the neighboring even-even nucleus. The low-lying levels are very sensitive to the nature of the collective states while the higher levels are much purer in structure. Thus a spectrum given on an absolute scale gives some indications of how well the structure of the collective states in an even-even nucleus are described while a spectrum given on a relative scale tends to hide this aspect.

#### A. $^{205}\text{Hg}$ nucleus

Little experimental work has been done on this nucleus. It has been studied mainly using ( $d, p$ ) reactions on  $^{204}\text{Hg}$  (see Refs. 13 and 14). Several levels were observed but there is a great uncertainty concerning the assignment of the spin and parity. Moreover, it seems that many states above 1.5 MeV excitation energy correspond to the coupling of a  $g_{9/2}$  neutron to states of  $^{204}\text{Hg}$ . These states are expected to be a 4h-1p structure and hence should not be described in our approach. As far as we know, from the theoretical point of view, nothing has been done since the old work of Lo Iudicé *et al.*<sup>15</sup> These authors used a weak-coupling basis with macroscopic phonons and drastically truncated their phonon space.

Quantitative comparison between the experimental spectrum and the KH and KR results is made in Table II. Only levels with some confidence concerning spin and parity are reported.

TABLE II. Comparison between experimental and theoretical spectrum of  $^{205}\text{Hg}$ . Only levels with some evidence for spin and parity are plotted. Energies are expressed in MeV with respect to the experimental ground state energy (for more details, see text).

$J^\pi$	Exp	KH	KR
$\frac{1}{2}^-$	0.0	-0.305	-0.842
$\frac{3}{2}^-$	0.381	0.192	0.049
$\frac{5}{2}^-$	0.469	0.301	0.088
$(\frac{7}{2}^+)$	1.855	1.972	
$(\frac{9}{2}^+)$	2.566	2.423	2.460
$(\frac{9}{2}^+)$	2.591	2.564	
$(\frac{5}{2}^+)$	2.920	2.966	
$(\frac{5}{2}^+)$	3.332	3.369	
$(\frac{5}{2}^+)$	3.488	3.438	
$(\frac{5}{2}^+)$	3.593	3.712	
$\frac{1}{2}^+$	3.838	3.786	
$\frac{1}{2}^+$	4.037	4.704	

The order of the three lowest states is correct with both interactions, but the calculated ground state energies are wrong by 305 keV using KH, and by 842 keV using KR. This disagreement is mainly due to the bad description of the  $0^+$  ground state of  $^{206}\text{Hg}$  which shows some deficiency of the proton hole-proton hole interaction—at least for  $0^+$  states. Curiously, the energies of the groups of  $\frac{3}{2}^+$  and  $\frac{5}{2}^+$  states observed in  $(d,p)$  reactions are rather well reproduced by shell-model calculations using the KH force, although it was expected<sup>13,14</sup> that they would be of a  $4h-1p$  type. The configuration space used for KR interaction is not large enough to allow the description of these states. Lastly, the first  $\frac{1}{2}^+$  state observed at 3.84 MeV seems to be the first calculated  $\frac{1}{2}^+$  state, while the second observed  $\frac{1}{2}^+$  at 4.04 MeV cannot be explained within our shell model calculation.

The whole spectrum below 1.7 MeV energy is shown on the left-hand side of Fig. 2 for both interactions. Based on the scarce experimental data it would seem that the KH force is much better than the KR one. On the right-hand side

of Fig. 2 we report the lowest states of given spin and parity above 2.5 MeV excitation energy calculated with the KH interaction. It appears that two levels are possible candidates for “yrast traps,” namely the  $\frac{23}{2}^-$  state at 3.49 MeV and the  $\frac{33}{2}^+$  state at 4.95 MeV. However, no definite conclusion can be drawn on that point since the order of the levels are rather sensitive to the force. Unfortunately the KR results are no help in that case because either the KR states are absent (configuration space not large enough) or the yrast KR states correspond in structure to states above the KH yrast line.

### B. $^{205}\text{Tl}$ nucleus

Because it is a stable nucleus,  $^{205}\text{Tl}$  has been the most studied and is correspondingly the most well known<sup>12</sup> among the nuclei considered in this paper. A number of states have been determined through various nuclear reactions<sup>16-20</sup> and electromagnetic properties have also been investigated.<sup>21-23</sup> Within the framework of WCM, but using macroscopic vibrational phonons, theoretical studies were carried out some time ago.<sup>8,24,25</sup> More recently new calculations were performed using a microscopic weak-coupling basis with three proton-hole orbits using only two collective phonons.<sup>7</sup>

The experimental spectrum and the corresponding states obtained by our exact shell model calculations are reported in Table III. The spectroscopic factors  $S_m = |\langle \psi_B | C_m(\text{proton}) | ^{206}\text{Pb}(0^+ \text{g.s.}) \rangle|^2$  for one proton transfer on  $^{206}\text{Pb}$  ground state are also indicated. In general the results obtained with the KH interaction are much better than those obtained with the KR interaction, especially for the spectroscopic factors. (A part of the discrepancy between experiment and theory for the low-energy part of the spectrum may be due to a bad description of the  $0^+$  ground state of  $^{206}\text{Pb}$ ; nevertheless, a bad proton-neutron interaction can also induce some incorrect order in the levels.)

Figure 3 shows the qualitative spectra, obtained with both interactions versus the experimental one. Only states with  $S_m > 0.01$  (with KH) are reported below 2 MeV. The correspondence with experimental levels is possible to make, thanks to the spectroscopic factors and the KH-KR correspondence, by examination of the wave functions. The order of the lowest levels is the same for both interactions and agrees with experiment. The deterioration for higher levels is mainly due to the poorness of the proton-neutron interaction. The right-hand side of the figure concerns the lowest states of a given spin and parity obtained using KH. Unfortunately the KR configuration space is not large enough to predict these states.

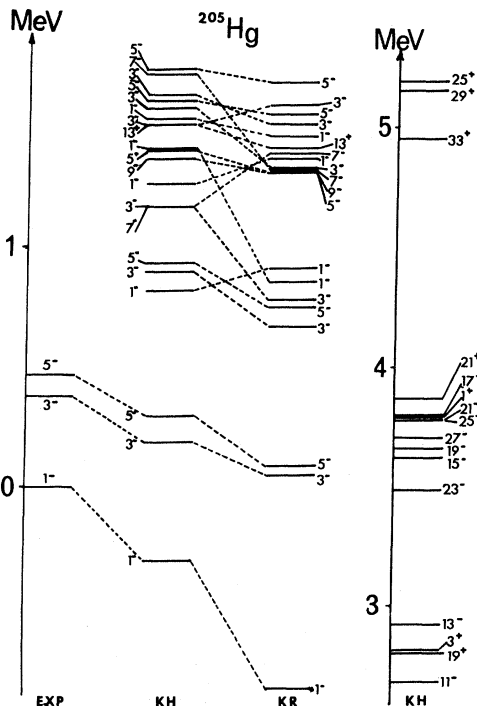


FIG. 2. Comparison between experimental and theoretical KH and KR spectra. The double of the spin is reported. Experimental data are taken from Ref. 12. All energies are referred to the experimental ground state. The correspondence between KH and KR levels is made by comparison of the wave function. In the right part of the figure, the lowest states of given spin and parity are drawn.

TABLE III. Same as Table II for  $^{205}\text{Tl}$ . The spectroscopic factor  $S$  is defined in the text.

$J^\pi$	Exp		KH		KR	
	$E$	$S$	$E$	$S$	$E$	$S$
$1/2^+$	0.0	0.70	-0.247	0.86	-0.514	0.96
$3/2^+$	0.204	0.40	0.086	0.66	0.102	0.79
$5/2^+$	0.619	0.05	0.519	0.08	0.614	
$7/2^+$	0.924		0.928	0.01	1.083	
$3/2^+$	1.141	0.20	0.847	0.19	0.655	0.11
$5/2^+$	1.180		1.032	0.08	0.970	
$1/2^+$	1.219	0.15	0.939	0.04	1.249	0.0
$3/2^+$	1.340	0.10	1.078	0.02	0.934	0.06
$(1/2)^+$	1.434	(0.15)	1.176	0.04	0.933	0.0
$11/2^-$	1.483	0.44	1.371	0.78		
$(5/2)^+$	1.866	(0.08)	1.607	0.16		
$(15/2^-)$	2.223		2.012			
$(7/2^-)$	2.487		2.022			
$(19/2^-)$	2.563		2.622			
$(5/2^-)$	2.623		2.441			
$(23/2^+)$	3.132		3.472			

An isomeric level at 3.13 MeV has been obtained<sup>26</sup> and on the grounds of a simplified shell-model calculation it has been assigned as a  $^{23}_2^+$  state. From our KH calculations this isomeric level could as well be a  $^{25}_2^+$  since the two corresponding theoretical states are close in energy. There might also be another trap here since our calculated  $^{35}_2^-$  state at 5.06 MeV is 0.2 MeV below the  $^{31}_2^-$  state and can only decay through  $E3$  transition to the  $^{29}_2^+$  state. Again this conclusion depends on the quality of the two-body KH interaction.

### C. $^{211}\text{Po}$ nucleus

Besides  $^{210}\text{Bi}$ , the  $^{211}\text{Po}$  and  $^{211}\text{Bi}$  nuclei are especially good samples for testing the particle proton-particle neutron effective interaction. Experimental data for these nuclei can be found in Ref. 27. The  $^{211}\text{Po}$  nucleus has been fruitfully investigated experimentally using mainly radioactivity<sup>28</sup> and nuclear reactions with neutrons,<sup>29</sup>  $\alpha$  particle,<sup>30</sup> and heavy ions.<sup>31</sup> With a one-proton orbit and one-neutron orbit, Auerbach and Talmi<sup>5</sup> have made some shell-model calculations for high-spin states. Since their paper, little, as far as we know, has been done from the theoretical point of view on this nucleus.

Comparison with experimental data is shown on Table IV. The spectroscopic factors  $S_1 = |\langle \psi_\beta | C_m^\dagger | \text{neutron } ^{210}\text{Po} (0^+ \text{ g.s.}) \rangle|^2$  correspond to a one-neutron transfer reaction from the  $^{210}\text{Po}$  ground state. The agreement between theory and experiment is quite good and curiously KR seems better for the energies and KH for the spectroscopic factors. An isomeric state with  $J > 19/2$  was reported in literature<sup>32</sup> at 1.463 MeV. From our calculation it is not conclusive whether it is a  $^{25}_2^+$  state (with KH) or a  $^{21}_2^+$  state (with KR) because these two levels are very close and the order is thus very sensitive to the two-body interaction.

Figure 4 shows the experimental and calculated spectra. Above 1 MeV excitation energy the level density becomes large and in order to keep the figure clear we reported only states with spectroscopic factors for one-nucleon transfer from  $^{210}\text{Po}$  ( $0^+$  g.s.) and  $^{210}\text{Bi}$  ( $1^+$  g.s.) greater than 0.01. The ground states energies are correctly given by KH as well as by KR. Moreover, the correspondence between the two spectra is better than it was for the previously studied nuclei. Although some levels may differ by some 300 keV, the level scheme is roughly the same with both interactions. The agreement with experimental energies is rather good and for this peculiar nucleus, KR energies seem better than KH ones. It is worthwhile noting that the KR parameters were fitted on  $^{210}\text{Po}$  for the proton-proton

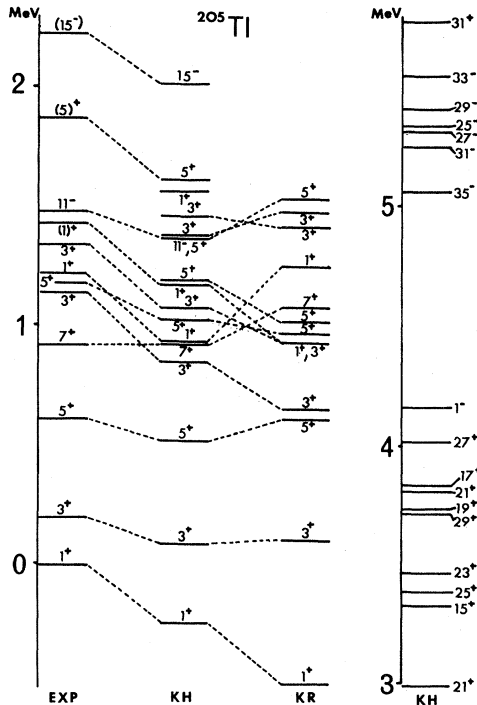


FIG. 3. Same as Fig. 2 for  $^{205}\text{Tl}$  nucleus. For the choice of reported theoretical levels, see text.

TABLE IV. Same as Table III for  $^{211}\text{Po}$ . S1 is defined in the text

$J^\pi$	Exp		KH		KR	
	E	S1	E	S1	E	S1
$\frac{9}{2}^+$	0.0	0.89	0.052	0.91	0.074	0.94
$\frac{11}{2}^+$	0.685	0.95	0.806	0.85	0.725	0.84
$\frac{5}{2}^+$	1.049	0.28	1.206	0.29	1.202	0.16
$(\frac{15}{2})^-$	1.065		1.245	0.77	1.168	0.78
$\frac{5}{2}^+$	1.378	0.08	1.693	0.01	1.495	0.0
$(\frac{5}{2})^+$	1.436	0.04	1.722	0.0	1.574	0.0
$\frac{5}{2}^+$	1.799	0.40	1.927	0.53	1.848	0.75
$\frac{1}{2}^+$	2.084	0.56	2.222	0.60	2.245	0.78
$(\frac{1}{2})^+$	2.161	0.20	2.696	0.10	2.453	0.02
$\frac{7}{2}^+$	2.606	0.29	2.689	0.20	2.554	0.19
$\frac{7}{2}^+$	2.639	0.12	2.793	0.17	2.676	0.17
$\frac{3}{2}^+$	2.661	0.13	2.264	0.11	2.411	0.05
$\frac{7}{2}^+$	2.862	0.32	2.911	0.18	2.780	0.36
$\frac{3}{2}^+$	2.910	0.51	2.683	0.33	2.758	0.66
$\frac{3}{2}^+$	3.252	0.22	2.963	0.18	3.213	0.12
$\frac{25}{2}^+$	1.463		1.643		1.573	
$\frac{21}{2}^+$			1.646		1.499	

interaction and on  $^{210}\text{Bi}$  for the proton-neutron interaction, thus it is not surprising that KR works well for the  $^{211}\text{Po}$ .

The right-hand side of the figure concerns the lowest states of given spin and parity. It is interesting to note that the KR interaction as well as the KH interaction predicts a  $\frac{31}{2}^-$  yrast trap around 2.4 MeV and a  $\frac{37}{2}^+$  isomeric state around 3.5 MeV.

#### D. $^{211}\text{Bi}$ nucleus

This nucleus is also very useful to test the proton-neutron interaction. Experimental studies<sup>32-35</sup> have been interpreted mainly in terms of the weak-coupling model. Some theoretical works have been developed but with drastic restrictions, two or three active orbits,<sup>6,36</sup> and/or few phonons taken into account.<sup>37,38</sup> As already pointed out the KR parameters used with configuration space of Fig. 1(b) are not at all suited for the description of  $^{210}\text{Pb}$  whose ground state is overbound by more than 600 keV. For this reason we decided to study  $^{211}\text{Bi}$  only with the KH interaction.

Many levels have been experimentally observed below 5 MeV excitation energy but assignment for spin and parity has only been made for a few of them. These states are reported in Table V with their measured spectroscopic factors  $S = |\langle \psi_\beta | C_{g\frac{9}{2}}^+ | \psi_{g\frac{9}{2}} \rangle|^2$

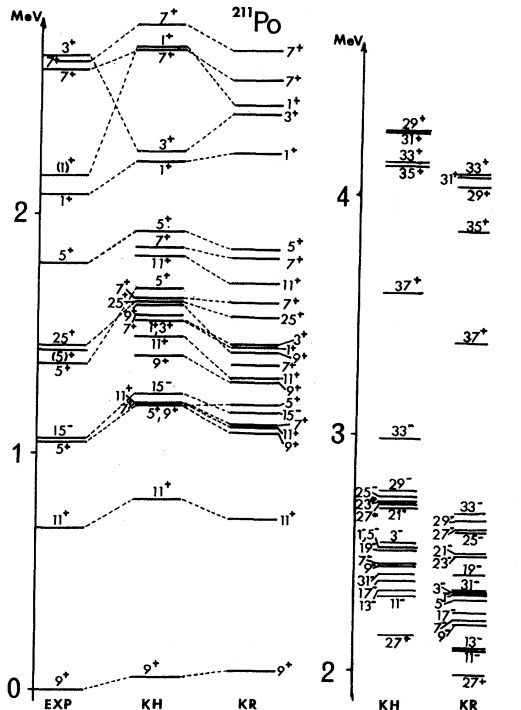


FIG. 4. Same as Fig. 3 for  $^{211}\text{Po}$  nucleus. Experimental data are taken from Ref. 27.

TABLE V. Same as Table III for  $^{211}\text{Bi}$ . Here  $S = |\langle \psi_\beta | C_{g\frac{9}{2}}^+ (\text{neutron})^{210}\text{Bi} (9^-) \rangle|^2$ . The spins and parities marked with an asterisk are not assigned experimentally but come from our calculations. For states marked with a double asterisk see comments in the text.

$J^\pi$	Exp		KH	
	E	$(2J_f+1)S$	E	$(2J_f+1)S$
$\frac{9}{2}^-$	0.0	$\leq 4.0$	0.123	5.57
$\frac{7}{2}^-$	0.405	$\leq 4.0$	0.760	
$\frac{11}{2}^-$	0.766	9	0.859	10.6
$\frac{9}{2}^-^{**}$	0.793	$\leq 4.0$	0.893	2.79
$\frac{13}{2}^-^{**}$	0.832	14	0.937	10.1
$(\frac{7}{2})^-$	1.014		0.997	
$(\frac{9}{2})^-$	1.109		1.079	0.15
$\frac{17}{2}^-^*$	1.118	20	1.230	16.1
$\frac{15}{2}^-^*$	1.136	18	1.237	15.2
$\frac{21}{2}^-^*$	1.217	25	1.320	22.9
$\frac{25}{2}^-^*$	1.257	42	1.322	37.5
$\frac{19}{2}^-^*$	1.270	21	1.372	18.6
$\frac{23}{2}^-^*$	1.398	21	1.473	17.7





not yet been observed experimentally.

As a result of our calculations, we are able to assign spins and parities to a group of levels in  $^{211}\text{Bi}$  for which only experimental energies are known. More complete results concerning theoretical energies, wave functions, and spectroscopic factors for both proton and neutron transfer are available on request.

#### ACKNOWLEDGMENTS

Very interesting and fruitful discussions with R. Liotta, F. Brut, and R. Piepenbring are greatly acknowledged. The authors are grateful to J. Sau for having provided a computer routine allowing diagonalization of large matrices with the Lanczos algorithm. We also thank R. Hilton for a careful reading of the manuscript.

- <sup>1</sup>A. de Shalit and I. Talmi, *Nuclear Shell Theory* (Academic, New York, 1963); Brussaard and Glaudemans, *Shell Model Applications in Nuclear Spectroscopy*, (North-Holland, Amsterdam, 1977).
- <sup>2</sup>J. B. Mc Grory and T. T. S. Kuo, Nucl. Phys. A247, 283 (1975).
- <sup>3</sup>C. M. Ko, T. T. S. Kuo, and J. B. Mc Grory, Phys. Rev. C 8, 2379 (1973); W. W. True and C. M. Ma, *ibid.* 9, 2275 (1974); D. Strottman, *ibid.* 20, 1150 (1979); P. Ring and P. Shuck, *ibid.* 16, 801 (1977).
- <sup>4</sup>J. P. Boisson, B. Silvestre-Brac, and R. J. Liotta, Nucl. Phys. A330, 307 (1979).
- <sup>5</sup>N. Auerbach and I. Talmi, Phys. Lett. 10, 297 (1964).
- <sup>6</sup>D. V. Rao and W. J. Gerace, Nucl. Phys. A175, 405 (1971).
- <sup>7</sup>L. Zamick, V. Klemm, and J. Speth, Nucl. Phys. A245, 365 (1975).
- <sup>8</sup>N. Azziz and A. Covello, Nucl. Phys. A123, 681 (1968).
- <sup>9</sup>T. T. S. Kuo and G. H. Herling, Naval Research Laboratory Report No. 2258 (Washington, DC, 1971).
- <sup>10</sup>Y. E. Kim and J. O. Rasmussen, Nucl. Phys. 47, 183 (1963).
- <sup>11</sup>Y. E. Kim and J. O. Rasmussen, Phys. Rev. 135, B44 (1964).
- <sup>12</sup>M. R. Schmorak, Nucl. Data Sheets, 23, 287 (1978).
- <sup>13</sup>M. L. Andersen, S. A. Andersen, O. Nathan, K. M. Bisgard, K. Gregessen, O. Hansen, S. Hinds, and R. Chapman, Nucl. Phys. A139, 17 (1970).
- <sup>14</sup>R. A. Moyer, Phys. Rev. C 5, 1678 (1972).
- <sup>15</sup>N. Lo Iudice, D. Prospero, and E. Salusti, Nucl. Phys. A127, 221 (1969).
- <sup>16</sup>C. Glashauser, D. L. Hendrie, and E. A. Mc Clatchie, Nucl. Phys. A222, 65 (1974).
- <sup>17</sup>N. Ahmed, D. R. Gill, W. J. Mc Donald, G. C. Neilson, and W. K. Dawson, Phys. Rev. C 11, 869 (1975).
- <sup>18</sup>E. R. Flynn, R. A. Hardekopp, J. D. Sherman, J. W. Sunier, and J. P. Coffin, Nucl. Phys. A279, 394 (1977).
- <sup>19</sup>P. A. Smith, Phys. Rev. C 18, 2486 (1978).
- <sup>20</sup>S. Hinds, R. Middleton, J. H. Bjerregaard, O. Hansen, and O. Nathan, Nucl. Phys. 83, 17 (1966).
- <sup>21</sup>M. Y. Chen, S. C. Cheng, W. Y. Lee, A. M. Ruskton, and C. S. Wu, Nucl. Phys. A181, 25 (1972).
- <sup>22</sup>W. Kratschner, H. V. Klapdor, and E. Grosse, Nucl. Phys. A201, 199 (1973).
- <sup>23</sup>O. Hausser, B. Haas, D. Ward, and H. R. Andrews, Nucl. Phys. A314, 161 (1979).
- <sup>24</sup>G. Alaga and G. Ialongo, Nucl. Phys. A97, 600 (1967).
- <sup>25</sup>A. Covello and G. Sartoris, Nucl. Phys. A93, 481 (1967).
- <sup>26</sup>I. Bergström, J. Blomqvist, G. G. Linden, O. Knuntilla, and T. Lonroth, Res. Inst. Phys. Stockholm Ann. Rep., 1976, p. 99.
- <sup>27</sup>M. J. Martin, Nucl. Data Sheets 25, 397 (1978).
- <sup>28</sup>L. J. Jardine, Phys. Rev. C 11, 1385 (1975).
- <sup>29</sup>T. S. Bhatia, T. R. Canada, P. D. Barnes, R. A. Eisenstein, and C. Ellegaard, Nucl. Phys. A314, 101 (1979).
- <sup>30</sup>T. Yamazaki, Phys. Rev. C 1, 290 (1970).
- <sup>31</sup>W. G. Davis, R. H. De Vries, G. G. Ball, J. S. Foster, W. C. Mc Latchie, D. Shapira, J. Toke, and R. E. Warner, Nucl. Phys. A269, 477 (1976).
- <sup>32</sup>S. Gorodetzki, F. A. Beck, T. Byrski, and A. Knipper, Nucl. Phys. A117, 208 (1968).
- <sup>33</sup>E. R. Flynn, D. G. Burke, J. D. Sherman, and J. W. Sunier, Nucl. Phys. A263, 365 (1976).
- <sup>34</sup>E. R. Flynn, R. E. Anderson, N. J. Di Giacomo, R. J. Petersen, and G. R. Smith, Phys. Rev. C 16, 139 (1977).
- <sup>35</sup>O. Hansen, J. P. Coffin, E. R. Flynn, N. Stein, and R. K. Sheline, Phys. Rev. C 18, 1223 (1978).
- <sup>36</sup>D. V. Rao and K. S. R. Sastry, Nucl. Phys. A175, 396 (1971).
- <sup>37</sup>A. M. Bradley and M. R. Meder, Phys. Rev. C 1, 1725 (1970).
- <sup>38</sup>W. Baldrige, N. Freed, and J. Gibbons, Phys. Lett. 46B, 341 (1973).
- <sup>39</sup>J. Blomqvist, private communication.
- <sup>40</sup>J. P. Schiffer and W. W. True, Rev. Mod. Phys. 48, 191 (1976).